Environmental Chemistry Letters (2018) 16:605–614
https://doi.org/10.1007/s10311-017-0701-8

ORIGINAL PAPER

High CO_2 adsorption by amino-modified bio-spherical cellulose nanofibres aerogels

Shuang Liu[1] · Yang Zhang[1] · Hua Jiang[2] · Xiaoyu Wang[1] · Tianmeng Zhang[1] · Yuan Yao[1]

Received: 8 October 2017 / Accepted: 22 December 2017 / Published online: 15 February 2018

Abstract

Climate change has become increasingly serious due to the greenhouse effect. It is therefore necessary to control the content of greenhouse gases such as carbon dioxide in the atmosphere, using, for instance, CO_2-adsorbing materials. Here, we synthesized ultra-lightweight and spherical cellulose nanofibres aerogels by a suspension titration method using an efficient amination process. These functional materials with high porosity, higher than 96.54%, and three-dimensional network structure, were prepared by freeze-drying spherical cellulose nanofibres hydrogel. Their maximum CO_2 adsorption capacity reaches 1.78 mmol/g, and they show excellent regeneration, of more than 10 cycles. This synthesis of bioaerogels represents a new method for the preparation of bio-CO_2 adsorbents.

Keywords Cellulose nanofibres · Cellulose nanofibres aerogels · Amine modification · Carbon dioxide (CO_2) adsorbents

Introduction

Since the industrial revolution, the increasing levels of carbon dioxide (CO_2), one of the primary greenhouse gases, has resulted in several environmental issues, such as climate change and global warming (Kerr 2007; Lais et al. 2017). Thus, it is essential to develop more research concerning the efficient capture and subsequent utilization of CO_2. The three conventional methods of current CO_2 capture technology involve (1) the adsorption method, (2) the membrane separation method, and (3) the low-temperature separation method (Chakraborty et al. 2002; Zhang et al. 2016). The adsorption separation method is attracting increasing attention because of its advantages, such as low-energy consumption, lack of corrosion, simple operation, and easy realization of automatic control (Rochelle 2009). However, most of the adsorbents have poor adsorption selectivity and low adsorption efficiency. To solve this problem, researchers have modified the adsorbents by grafting and dipping. One of the best modifications is that with an aminating agent. Through the amine modification, the adsorbent has excellent adsorption selectivity, which further improves the adsorption efficiency and increases the adsorption capacity of the adsorbent. For example, after modification by polyethylenimine (PEI) and other aminating agents, the CO_2 adsorption performance of Santa Barbara Amorphous-16 (SBA-16) and other mesoporous materials is significantly enhanced (Kim et al. 2005; Chen et al. 2013; Vilarrasa-Garcia et al. 2015). The PPN-6CH_2DETA adsorbent is obtained by grafting diacetamide (DETA) onto the polymer PPN-6 (PPN stands for porous polymer networks). PPN-6 is a covalently bonded carbon scaffold with a Brunauer-Emmett-Teller (BET) surface area of 4023 m^2/g, which is extremely stable towards strong acid and base). This new adsorbent's selectivity to carbon dioxide adsorption is 3.6×10^{10} (Lu et al. 2013). However, these conventional adsorbents have several drawbacks, such as secondary pollution to the environment, raw materials shortage, and complex synthesis methods.

In the context of a sustainable society, several criteria should be met for a material to be used as a CO_2 absorbent, including a high CO_2 absorption capacity and CO_2 selectivity, a fast CO_2 adsorption rate, high floatability (hence a low density), low cost, environmental friendliness, and excellent recyclability.

As a new generation of bioaerogels, cellulose aerogels show excellent characteristics. This material not only has

✉ Yang Zhang
yangzhang31@126.com

[1] College of Materials Science and Engineering, Nanjing Forestry University, Nanjing 210037, People's Republic of China

[2] College of Chemical Engineering, Nanjing Forestry University, Nanjing 210037, People's Republic of China

the advantages of traditional aerogels, including lightweight, high porosity, high specific surface area, and low dielectric constant (Shlyakhtina and Oh 2008), but also has its own unique advantages, such as low cost and high availability of raw materials, biocompatibility, and biodegradability (Huang et al. 2006). These properties are the reasons why bioaerogels from cellulose have been developed during the past decade (Cai et al. 2008; Gavillon and Budtova 2008; Sehaqui et al. 2011b), using cellulose derivatives (Fischer et al. 2006; Silva et al. 2012; Chen et al. 2014) or cellulose nanofibres (Zheng et al. 2014; Víctor-Román et al. 2015; Zheng et al. 2016).

In recent years, cellulose aerogels have been widely studied as adsorbents. In terms of oil absorption, the researchers obtained a highly oil-absorbing material by hydrophobizing ultra-lightweight and highly porous cellulose aerogels, and they can collect a wide range of organic solvents and oils with absorption capacities up to many times their own weight (Zhang et al. 2014; Jin et al. 2015). Recent studies have shown that nanofibrillated cellulose sponges could absorb up to 45 times their own weight in organic solvent or oil, depending on the liquid (Cervin et al. 2012). In the case of gas adsorption, the cellulose aerogels are modified by cross-linking with PEI. The composite cellulose aerogels obtained have an excellent CO_2 adsorption capacity (Sehaqui et al. 2015). It can be foreseen that cellulose aerogels have great potential as a bio-adsorbent. In the current work, in order to obtain a green CO_2 absorbent with high absorption capacity, we prepared the cellulose nanofibres by the chemical mechanical method, which uses eucalyptus pulp as a raw material. Next, the spherical cellulose nanofibres hydrogel was obtained by the suspension titration method. Finally, the amino-modified bio-spherical cellulose nanofibres aerogels were prepared with the freeze-drying technology and grafting modification method. The new materials have been evaluated in terms of morphology, structure, and CO_2 adsorption performance.

Experimental section

Materials

Eucalyptus pulp was provided by a paper mill (Jiangsu, China). Potassium hydroxide (KOH) and sodium chlorite ($NaClO_2$) were received from Nanjing Chemical Reagent Co., Ltd. Glacial acetic acid (≥ 99.0%), *tert*-butanol (≥ 99.5%), calcium chloride ($CaCl_2$), and hydrochloric acid (HCl) (36–38%) were of analytical grade, and they were all purchased from Nanjing Chemical Reagent Co., Ltd. *N*-(2-Aminoethyl)(3-aminopropyl)methyldimethoxysilane (AEAPMDS) (≥ 97%) was supplied by Alfa Aesar (UK). Distilled water was used in all experiments.

Preparation of cellulose nanofibres

In this experiment, 10 g of KOH was added to a beaker with the flocculent eucalyptus pulp and 500 mL of distilled water. The beaker was placed at an electrical agitator for 2 h at 90 °C. The resulting mixture was filtered to neutral. Subsequently, the filtered pulp was put into a beaker containing 400 mL of distilled water, 12 mL of glacial acetic acid, and 30 g of sodium chlorite. The mixed solution was agitated with an electrical agitator for 5 h at 80 °C. The aqueous suspension filtered to neutral was introduced into 500 mL of distilled water, and 20 g of KOH was added. The aqueous suspension was agitated with an electrical agitator for 2 h at 90 °C. After the resulting suspension was filtered to neutral, the suspension obtained was added to a 400 mL beaker with 12 mL of HCl. After the solution was subjected to a chemical reaction for 2 h at 80 °C, the solution was again filtered to neutral. Finally, the cellulose suspension obtained was high ground 6–8 times by Supermasscolloider Medium attritor (MKZA15-40J). The cellulose nanofibres suspension was obtained according to the published literature (Zhang et al. 2015; Zhao et al. 2015); then, it was centrifuged and the solid content was measured.

Synthesis of unmodified and amino-modified bio-spherical cellulose nanofibres aerogels

The cellulose nanofibres obtained as described above were formulated as a 2% cellulose nanofibres hydrosol. After ultrasonic freezing for 40 s and standing for 5 min, the spherical cellulose nanofibres hydrogel was prepared by titrating the hydrosol to a specific concentration of $CaCl_2$ solution which can promote gelation of cellulose nanofibres.

The same amount of spherical cellulose nanofibres hydrogel was introduced into beakers containing an aqueous solution of AEAPMDS with a mass fraction of 0, 3, 4, and 5%, respectively. These beakers were placed in water baths at 80 and 90 °C for 10 h. Subsequently, the solution was displaced by *tert*-butanol alcohol. After 24 h, unmodified and AEAPMDS-modified bio-spherical cellulose nanofibres aerogels were obtained by freeze-drying. Finally, the AEAPMDS-modified bio-spherical cellulose nanofibres aerogels were denoted as 0-80-aerogel, 3-80-aerogel, 4-80-aerogel, 5-80-aerogel, 0-90-aerogel, 3-90-aerogel, 4-90-aerogel, and 5-90-aerogel. 0, 3, 4, and 5 indicate that the mass fraction of the AEAPMDS solution is 0, 3, 4, and 5% correspondingly; 80 and 90 mean that the temperatures of the chemical reactions were at 80 and 90 °C, respectively.

Structure, physical, and chemical properties testing

The AJSE-7600 JEOL scanning electron microscope (SEM) operating at 15 kV was used to capture structural images

of the bio-spherical CNF aerogels. Images were taken at magnifications of 2000×, 5000×, 10,000×, and 20,000×. The structural images of the cellulose nanofibres were tested by transmission election microscope (TEM) analysis. The change of functional groups of amino-modified bio-spherical cellulose nanofibres aerogels could be investigated and compared with unmodified spherical cellulose nanofibres aerogels by Fourier-transform infrared spectroscopy (FTIR) (model: Nicolet 360, Thermo, USA). The thermal stability of the bio-spherical cellulose nanofibres aerogels was studied by thermogravimetric analysis (TGA). The nitrogen content of bio-spherical cellulose nanofibres aerogels was obtained by the EA3000 Elemental Analyser. Nitrogen adsorption–desorption isotherms was obtained using a surface area and pore size analyser (accelerated surface area porosimetry 2020 (ASAP 2020) Analyser Micromeritics, USA). The curve of the TG data was plotted using the software Origin 8.0. TG analysis was carried out on Netzsch 409PC thermogravimetric analyser.

Evaluation of the density and porosity of bio-spherical cellulose nanofibres aerogels

The apparent volumetric mass density of the bio-spherical cellulose nanofibres aerogels was calculated by dividing their weight by their volume, as in the following formula:

$$\rho_{\text{aerogels}} = \frac{m}{V} \tag{1}$$

where m and V are the weight and volume of the bio-spherical CNF aerogels, respectively.

The porosity was calculated using the following equation:

$$\varepsilon = \left(1 - \frac{\rho_{\text{aerogels}}}{\rho_{\text{s}}}\right) \times 100\% \tag{2}$$

where ρ_{aerogels} and ρ_{s} are the volumetric mass densities of AEAPMDS-treated cellulose nanofibres aerogels and densities of the solid scaffold (cellulose or AEAPMDS-treated cellulose), respectively.

Considering that the AEAPMDS-treated cellulose nanofibres aerogels can be regarded as composite cellulose aerogels, ρ_{s} was calculated according to Eq. (3), which was similar to the formula from the literature for modified cellulose aerogels (Zhang et al. 2014):

$$\rho_{\text{s}} = \frac{1}{\frac{w_{\text{cellulose}}}{\rho_{\text{cellulose}}} + \frac{w_{\text{AEAPMDS}}}{\rho_{\text{AEAPMDS}}}} = \frac{1}{\frac{1-w_{\text{AEAPMDS}}}{\rho_{\text{cellulose}}} + \frac{w_{\text{AEAPMDS}}}{\rho_{\text{AEAPMDS}}}} \tag{3}$$

where $w_{\text{cellulose}}$ is the weight fraction of cellulose in the AEAPMDS-modified bio-spherical cellulose nanofibres aerogels and w_{AEAPMDS} is the weight fraction of AEAPMDS. $\rho_{\text{cellulose}}$ was fixed at 1.60 g/cm^3 (Ganster and Fink 2003), and ρ_{AEAPMDS} was at 0.94 g/cm^3.

w_{AEAPMDS} was calculated according to Eq. (4):

$$w_{\text{AEAPMDS}} = \frac{w_{\text{N}}}{w} \tag{4}$$

where w_{N} is nitrogen content in the AEAPMDS-modified bio-spherical cellulose nanofibres aerogels (shown in Fig. 2) and w is the weight fraction of nitrogen in the AEAPMDS with a value of 15.91%.

Carbon dioxide (CO_2) adsorption performance test

The adsorption capacity of the cellulose nanofibres aerogels was obtained by custom-built adsorption test device (shown in Fig. 1A). The adsorption performance of the adsorbent was measured by the static method (Chen et al. 2016). The experiment was carried out as follows.

After the airtightness of the detecting device was ensured, the dried bio-spherical cellulose nanofibres aerogels were placed in the adsorbent bed 4. Next, opening the vacuum pump and all of the valves (except the valve $v7$ and the pressure reducing valve $v1$), the entire apparatus was changed to a low-pressure state to remove the internal residual air. Subsequently, the valves ($v3$, $v4$, $v6$) and vacuum pump were closed, other valves ($v7$, $v1$) were opened, and a sufficient amount of pure carbon dioxide gas was introduced into control tank 5. Next, the needle valve $v2$ was closed. After stabilizing, the displayed pressure and the temperature were denoted as $P1$ and $T1$ at this time. The needle valves ($v3$, $v4$) were subsequently opened to introduce carbon dioxide gas into the adsorption bed, which carried out the static method to test the adsorption performance of the adsorbent. Time and pressure were recorded every 5 min. When the pressure gauge and the thermometer no longer showed changes, it proved that the adsorption reached equilibrium, and the pressure ($P2$) and the temperature ($T2$) were recorded at this time. The maximum adsorption capacity of the adsorbent was calculated by Eq. (5) (the $v1$–$v7$ described above represented different valves, respectively):

$$N = \frac{\frac{P1V1}{RT1} - \frac{P2V2}{RT2}}{m} \tag{5}$$

where $V1$ is the total volume of all pipes between two $v2$ and $v6$, except for the volumes of the pipes between $v3$ and $v4$, including volume of the control tank 5. $V2$ is the total volume of all pipes between $v2$ and $v6$, including the volumes

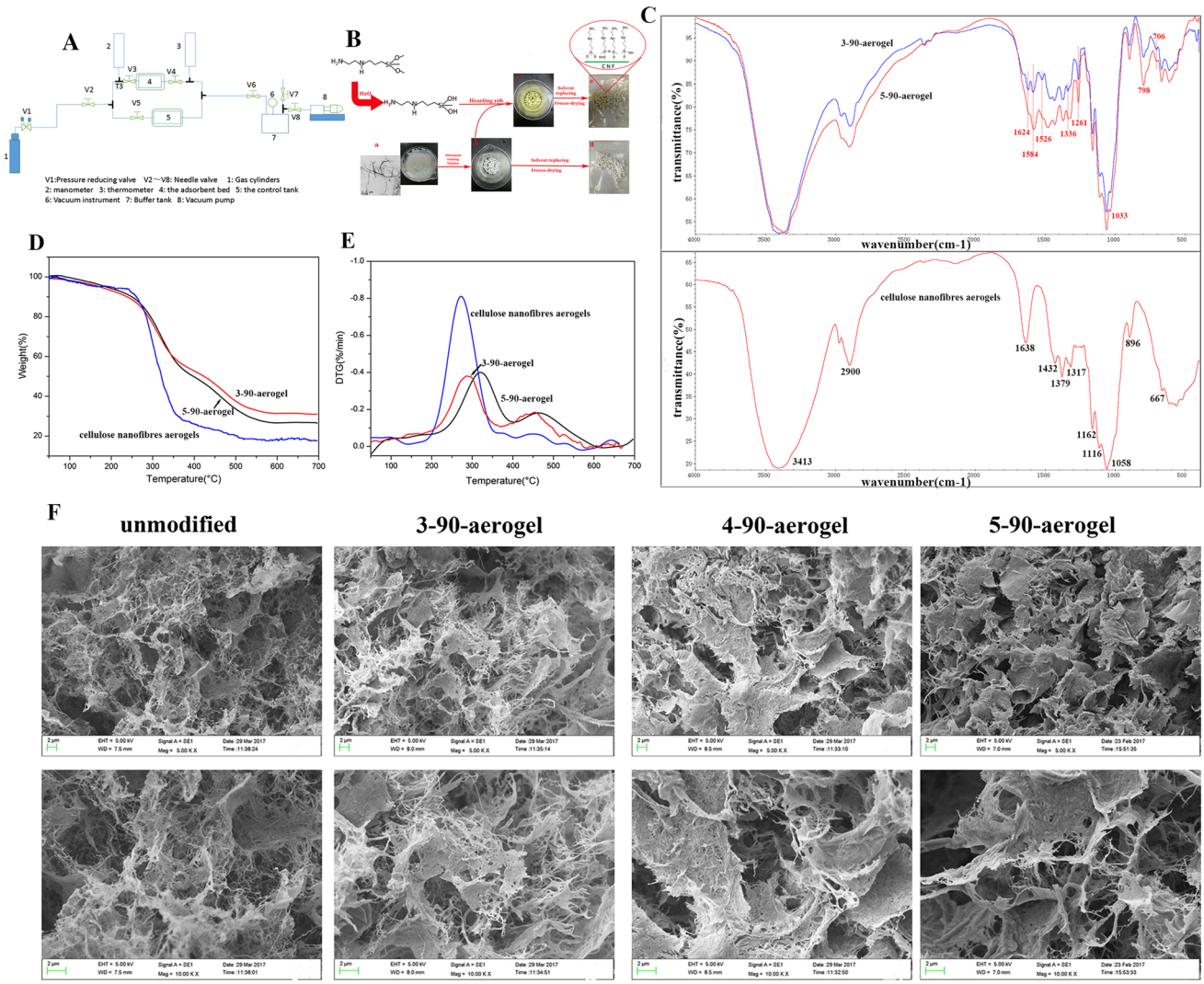

Fig. 1 **A** Structure diagram of custom-built adsorption test device. **B** General scheme for the synthesis of amino-modified bio-spherical cellulose nanofibres aerogels. The chemical structure of AEAPMDS (*N*-(2-aminoethyl)(3-aminopropyl)methyldimethoxysilane). (a) Image and transmission electron microscope (TEM) micrograph of cellulose nanofibres. (b) Image of unmodified bio-spherical cellulose nanofibres hydrogel. (c) Image of bio-spherical cellulose nanofibres hydrogel. (d) Image of bio-spherical cellulose nanofibres aerogels. (e) Image of amino-modified bio-spherical cellulose nanofibres aerogels. **C** The infrared spectra of the amino-modified bio-spherical cellulose nanofibres aerogels. **D** Thermogravimetric analysis (TG) curves of the amino-modified bio-spherical cellulose nanofibres aerogels. **E** Differential thermal gravity (DTG) curves of the amino-modified bio-spherical cellulose nanofibres aerogels. **F** Scanning electronic microscopy (SEM) micrographs of the amino-modified bio-spherical cellulose nanofibres aerogels

of the control tank 5 and = adsorbent bed 4. *m* is the quality of the bio-spherical cellulose nanofibres aerogels.

The regenerability test of the cellulose nanofibres aerogels was performed by the home-made adsorption test device. After the adsorption test was completed, the sample was desorbed at 150 °C for 48 h. Then, the desorbed sample was replaced in the test device. The CO_2 adsorption performance of the samples was tested again according to the above method, and the CO_2 adsorption capacity was calculated; this was repeated for 10 cycles.

Results and discussion

Structure, physical, and chemical properties of the amino-modified bio-spherical cellulose nanofibres aerogels

Cellulose nanofibres were isolated from the eucalyptus pulp using the chemical mechanics method. TEM analysis of the resulting cellulose nanofibres suspension revealed the microstructure of cellulose nanofibres, which was similar to long sticks with diameters in the nanometre range and lengths

in the micron range (as shown in Fig. 1B-a). After ultrasonic freezing and standing, the morphological structure of the spherical cellulose nanofibres hydrogel obtained by the suspension titration method was a white sphere (Fig. 1B-b). It became a pale yellow sphere after the spherical cellulose nanofibres hydrogel reacted with AEAPMDS for ten hours (Fig. 1B-c). The material turned into a white spherical solid and pale yellow spherical solid, respectively, after freeze-drying (Fig. 1B-d, e). As shown in the image, adding the modifier had almost no effect on the shape of the bio-spherical cellulose aerogels. However, only the colour of the cellulose nanofibres aerogels has changed.

The SEM images of the amino-modified bio-spherical cellulose nanofibres aerogels are displayed in Fig. 1F. The internal structure of both unmodified and amino-modified bio-spherical cellulose nanofibres aerogels displayed three-dimensional network structures composed of film-like structures and fibre silks. The film-like structure seemed to be caused by the coagulation of the fibrils during the freezing process (Jin et al. 2004; Svagan et al. 2008; Sehaqui et al. 2011a). Compared with unmodified bio-spherical cellulose nanofibres aerogels, the film-like structure of the amino-modified bio-spherical cellulose nanofibres aerogels was more evident, and the number of structures increased with higher AEAPMDS percentages. This could be the reason that AEAPMDS could connect the fibrils. Therefore, we observed that the porous structure of the 5-90-aerogel was almost entirely composed of the film-like structure. This finding indicated that the network structure of the bio-spherical cellulose nanofibres aerogels could be affected by the modifier, and AEAPMDS accessed the cellulose nanofibres aerogels successfully.

The infrared spectra of amino-modified bio-spherical cellulose nanofibres aerogels are shown in Fig. 1C. The absorption peaks of the spherical cellulose nanofibres aerogels had obvious characteristic absorption peaks of cellulose macromolecules, the absorption peak at 3413 cm^{-1} was OH stretching vibrations, near 2900 cm^{-1} was assigned to CH stretching, CH_2 symmetric bending at 1432 cm^{-1}, OH and CH bending as well as C–C and C–O stretching appeared at 1379, 1317, 1116 and 1162 cm^{-1} was assigned to C–O–C asymmetric stretching vibration from the glycosidic ring, 1058 cm^{-1} was attributed to C–O symmetric stretching, CH out of bending vibration was assigned to 896 cm^{-1}, and OH out of plane bending was at 667 cm^{-1} (Fu et al. 2016), which indicated that the amino-modified bio-spherical cellulose nanofibres aerogels still retained the internal structures of cellulose after the modification and heating process. Thus, they were still cellulose-based materials.

However, from Fig. 1C, we could see the following differences. (1) The unmodified spherical cellulose nanofibres aerogels had a strong absorption peak at 1638 cm^{-1}, which was the O–H bending vibration peak of the surrounding water absorbed by the cellulose (Shi et al. 2013). In contrast, this absorption peak of the amino-modified spherical cellulose nanofibres aerogels was weak. There may be reasons that the hydrophilic of the modified aerogels was weaker than the unmodified cellulose nanofibres aerogels (Abdelmouleha et al. 2004; Gebald et al. 2011). (2) Compared with the unmodified spherical cellulose nanofibres aerogels, the AEAPMDS-modified bio-spherical cellulose nanofibres aerogels showed new absorption peaks, such as the NH^{3+} deformation at 1624 cm^{-1} (Mohammed et al. 2011) and N–H bending of the NH_2 group at 1584 and 1482 cm^{-1} (Abdelmouleha et al. 2004; Niu et al. 2016). Simultaneously, the band at 1336 cm^{-1} was attributed to the C–N stretching vibration peak, the band near 1261 cm^{-1} the Si–C stretching vibration peak (Knöfel et al. 2009; Gebald et al. 2011), the band near 1033 cm^{-1} was attributed to the stretching vibration peak of Si–O–cellulose and the band at 798 and 706 cm^{-1} were assigned to the Si–O–Si stretching vibration peak (Lu et al. 2008; Fu et al. 2016). The grafting conditions employed herein were sufficient for covalent bonding of silane molecules, as corroborated by the appearance of signals associated with vibrations from silicon-based linkages at 1261 cm^{-1}, 1033 cm^{-1}, 798 cm^{-1} and 706 cm^{-1}.

The thermal stability of the bio-spherical cellulose nanofibres aerogels was investigated by TG-DTG (Fig. 1D, E). The bio-spherical cellulose nanofibres aerogels modified by different AEAPMDS percentages was tested from 0 to 700 °C under N_2. The weight loss of the material below 150 °C could be attributed to removing the physically adsorbed water and the small amount of CO_2 in the air. In the range of 300–600 °C, a sharp and narrow peak was observed, indicating an intense reaction (Fig. 1D). This stage accounted for most of the entire weight loss, which is due to releasing considerable gas (CO_2 and H_2O) because of the thermal degradation of the cellulose nanofibres aerogels. Simultaneously, the loss weight of the unmodified spherical cellulose nanofibres aerogels was more than that of the modified cellulose nanofibres aerogels. It may be that the thermal degradation of AEAPMDS in the modified cellulose nanofibres aerogels produced new substance, such as SiO_2. This again confirmed the successful modification of the cellulose nanofibres aerogels.

From Fig. 1E, the temperature of the maximum weight loss rate (T_{max}) of the unmodified bio-spherical cellulose nanofibres aerogels was lower than that of the modified ones, and with AEAPMDS percentage increased, T_{max} increased (272.57, 288.46, and 318.84 °C were the T_{max} values of the 0-90-aerogel, 3-90-aerogel, and 5-90-aerogel, respectively). This might be because bio-spherical cellulose nanofibres aerogels were modified by AEAPMDS, which increased the T_{max} value, and it indicated that the amination of the cellulose nanofibres aerogels could improve their thermal stability to some extent.

Adsorption performance of the amino-modified bio-spherical cellulose nanofibres aerogels

The adsorption mechanism of the amino-modified adsorbent adsorbing carbon dioxide mainly occurred in the following three ways (Sharma et al. 2012; Zhang et al. 2012):

$$CO_2 + 2RNH_2 \rightarrow RNHCOO^- + RNH_3^+ \quad (6)$$

$$CO_2 + 2R_2NH \rightarrow R_2NHCOO^- + R_2NH_2^+ \quad (7)$$

$$CO_2 + R_2NH + R'NH_2 \rightarrow R_2NCOO^- + R'NH_3^+ \quad (8)$$

The nitrogen content was very important to the carbon dioxide adsorbent. The percentage of nitrogen in the AEAPMDS-modified bio-spherical cellulose nanofibres aerogel was examined by EA3000 (Table 1). The maximum *N* content in the modified cellulose aerogels reached 5.482%, and the nitrogen content was positively correlated with the temperature (≤ 90 °C) and the mass fraction of AEAPMDS (≤ 5%). This finding confirmed that the composite cellulose nanofibres aerogels were well integrated with the modifier, which was likely to have selective adsorption of carbon dioxide.

The diameter, volumetric mass density, porosity, and specific surface area of unmodified and amino-modified bio-spherical cellulose nanofibres aerogels are listed in Table 1. The diameter was measured by calculating the average diameter of 50 bio-spherical cellulose nanofibres aerogels, and the measured porosities and densities were consistent with data from the literature for bioaerogels (Aulin et al. 2008; Sehaqui et al. 2010). The specific surface area, pore size, and pore volume were obtained by the BET method. Ultralightweight and highly porous (≥ 96%) amino-modified bio-spherical cellulose nanofibres aerogels were obtained. The diameter of the bio-spherical cellulose nanofibres aerogels basically remained the same; a gradual decrease in porosity and a gradual increase in density were noted with an increase in the mass fraction of AEAPMDS and the temperature. These illustrated that amine modification did not affect the shape of the spherical cellulose nanofibres aerogels, and the density and porosity of the cellulose nanofibres aerogels decreased due to the ingestion of the aminating agent. From the table, we could see that the pore size, surface area, and pore volume of the unmodified cellulose nanofibres aerogels were smaller than those of the modified cellulose nanofibres aerogels, probably because of the AEAPMDS embedded into the pores of the cellulose nanofibres aerogels.

The adsorption capacity of the amino-modified bio-spherical cellulose nanofibres aerogels was obtained by a homemade detection device at an initial pressure (0.135 MPa) and room temperature (20 °C) (shown in Table 1). The modified cellulose nanofibres aerogels had a higher CO_2 adsorption capacity than the unmodified samples, which was mainly due to the high nitrogen content of the modified cellulose aerogels. The adsorption capacity of aerogels obtained at 90 °C was higher than that of 80 °C; the higher the nitrogen content, the higher the adsorption capacity. From Fig. 2A, the amino-modified bio-spherical cellulose nanofibres aerogels had a higher adsorption efficiency, and it took only approximately 30 min to reach the maximum adsorption capacity. This could be the reason that the beginning stage shows a sharp linear weight gain due to the surface chemical reaction, and the second stage involves a comparatively slow physical diffusion (Liu et al. 2014). According to the calculation with Eq. (5), the adsorption capacity of the 5-90-aerogel reached 1.78 mmol/g. This capacity was more than the adsorption capacity of the first stage grafted modified CO_2 adsorbent (Hiyoshi et al. 2005; Khatri et al. 2005) and higher than the adsorption capacity of some carbon dioxide adsorbents reported in the literature (Niu et al. 2016). This could be reason that the high efficiency of the coupling between AEAPMDS and bio-spherical cellulose nanofibres aerogels made the amine content higher.

Table 1 Structural property of the amino-modified bio-spherical cellulose nanofibres aerogels

Sample	The average diameter (mm)	Density (g/cm^3)	ρ_s (g/cm^3)	Porosity (%)	BET surface area (m^2/g)	Pore volume (cm^3/g)	Pore size (nm)	*N* content (%)	Adsorption capacity (mmol/g)
0-80-aerogel	5.519	0.0234	1.60	98.54	52.4	0.216	16.5	0	0.34
3-80-aerogel	5.412	0.0252	1.40	98.20	31.8	0.169	21.2	3.198	1.13
4-80-aerogel	5.452	0.0323	1.36	97.63	34.5	0.172	19.8	3.796	1.25
5-80-aerogel	5.503	0.0368	1.34	97.25	32.4	0.184	22.7	4.464	1.36
0-90-aerogel	5.489	0.0229	1.60	98.43	55.6	0.239	17.0	0	0.28
3-90-aerogel	5.509	0.0278	1.39	98.00	30.4	0.165	20.6	3.886	1.28
4-90-aerogel	5.505	0.0369	1.33	97.23	36.2	0.183	19.6	4.668	1.45
5-90-aerogel	5.495	0.0446	1.29	96.54	36.4	0.177	19.4	5.482	1.78

BET Brunauer-Emmett-Teller

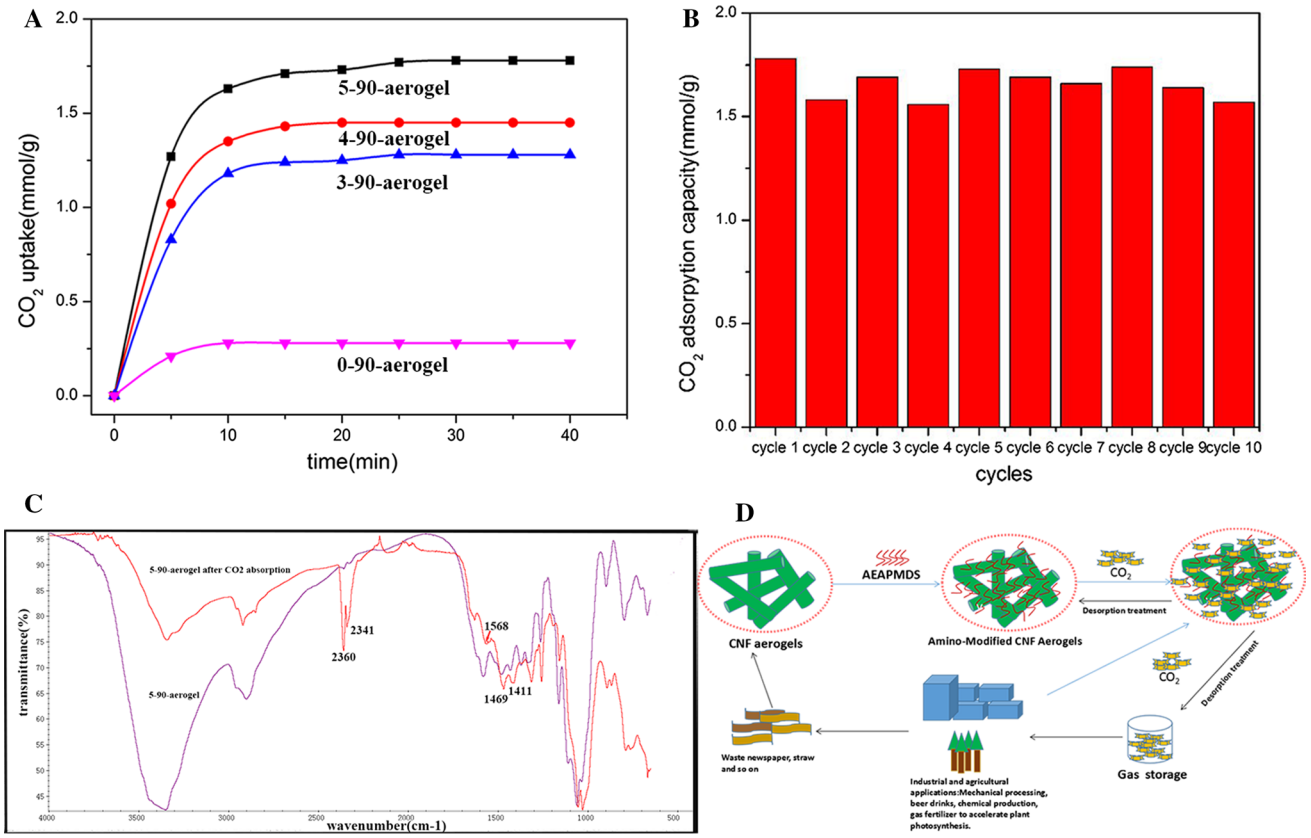

Fig. 2 **A** CO_2 isotherms of the amino-modified bio-spherical cellulose nanofibres aerogels at 20 °C. **B** Cyclic stability of 5-90-aerogel adsorption conditions: T = 20 °C, m = 0.12 g; desorption conditions: T = 150 °C, time = 48 h. **C** The infrared spectra of amino-modified bio-spherical cellulose nanofibres aerogels after CO_2 adsorption. **D** Design diagram for amino-modified bio-spherical cellulose nanofibres aerogels industrial circulation application patterns

The infrared spectrum of amino-modified bio-spherical cellulose nanofibres aerogels after CO_2 adsorption is shown in Fig. 2C. Near 2360 and 2341 cm^{-1} were attributed to C=O vibration, which was caused by unreacted CO_2 inside the CNF aerogels. This showed that the aerogels underwent physical adsorption process which was reason that unmodified aerogel had a certain adsorption capacity (shown in Fig. 2A). And band at 1568 cm^{-1} resulted from the asymmetric stretching vibration of $(N)COO^-$, and near 1469 cm^{-1} was ascribed to NH^{3+} deformation vibration and the band at 1411 cm^{-1} to $(N)COO^-$ symmetric stretching vibration (Bacsik et al. 2011; Gebald et al. 2011; Danon et al. 2016). These indicated that CO_2 reacted with the amino groups in the modified cellulose nanofibres aerogels to form carbamic acid and carbamates, as noted above for the reaction mechanism of the solid amine adsorbents, which confirmed that the chemisorption of the amino-modified bio-spherical cellulose nanofibres aerogels took place.

Excellent adsorption materials not only need to have a large adsorption capacity but also must be reusable, that is, after several adsorption and desorption events, the material adsorption capacity should not change significantly. Therefore, the 5-90-aerogel had been evaluated for several cycles of adsorption and desorption by a home-made detection device. The adsorption capacity of the 5-90-aerogel is shown in Fig. 2B. After 10 cycles of adsorption and desorption, the adsorption capacity of the 5-90-aerogel did not change significantly (from 1.52 to 1.78 mmol/g). This indicated that the 5-90-aerogel has good adsorption and desorption cycle stability and further confirmed that the link between the bio-spherical cellulose nanofibres aerogels and AEAPMDS was a combination of chemical bonds. Compared with the adsorbent, which was susceptible to deactivation after repeated cycles of desorption, this material had a higher surface thermal stability. Therefore, it is an adsorbent with potential industrial applications.

In addition, Table 2 provides a comparison of the reported CO_2 adsorbents with our amino-modified bio-spherical cellulose nanofibres aerogels. From Table 2, the supporting materials of these samples generally needed a complex synthesis process or a high cost. Simultaneously, the raw material of some samples is scarce. Some adsorbents may also cause pollution to the environment, and it was difficult

Table 2 Comparison of different samples for CO_2 capture under dry conditions

Sample	Support	Amine	CO_2 capacity (mmol/g)	Temperature (°C)	References
Silicagel–PEI-50	Silicagel	PEI	1.775	40	Xu et al. (2003)
30 PEI/bentonite	Bentonite	PEI	1.1	75	Vilarrasa-Garcia et al. (2015)
C-APTMS-PEI	Montmorillonite nanoclay	APTES + PEI	1.7	85	Roth et al. (2013)
HNTS-NH_2	Halloysite	APTES	0.13	25	Kim et al. (2016)
HP20/PEI	Resin	PEI	1.92	75	Chen et al. (2013)
Carbon–DETA	Carbon	DETA	0.91	20	Plaza et al. (2007)
TA/SBA-15	SBA-15	TA	1.58	60	Hiyoshi et al. (2005)
5-90-aerogel	Cellulose nanofibres aerogels	AEAPMDS	1.78	20	This work

APTMS 3-aminopropyltrimethoxysilane; *HNTS* halloysite nanotubes; *APTES* (3-aminopropyl) triethoxysilane; *HP20* 20% Hep; *DETA* diacetamide; *TA* (3-trimethoxhysilylpropyl)diethylenetriamine

to address them. The application of silicone solid in this field has also attracted attention recently. The bottom half of Table 2 shows some works using silicone solid used the supporting material, such as SBA-15, mobil composition of matter No. 48 (MCM-48), and SBA-16. Compared with these reports, our amino-modified bio-spherical cellulose nanofibres aerogels displayed better adsorption properties. The bio-spherical cellulose nanofibres aerogels can be made from open crop straw, and these open crop straws are burned each year in China (Mehmood et al. 2017). So the preparation of bio-spherical cellulose nanofibres aerogels can not only increase the utilization of crop straws, but also indirectly reduce release of particulate matter (PM) and gaseous pollutants. However, the material prepared also had some defects: its strength was low, and it was easy to be crushed and deformed; the preparation process need to vacuum freeze-dried, thus raising the cost; and the preparation of nanocellulose was also relatively complicated. Therefore, we still need to further explore the preparation of this material, such as adding enhancer to increase its strength, trying to dry at atmospheric pressure or other drying methods, and exploring material preparation conditions (reaction time, temperature, the amount of AEAPMDS) to find the best preparation process.

Through the above results, design diagram for amino-modified bio-spherical cellulose nanofibres aerogels industrial circulation application patterns is shown in Fig. 2D. Amino-modified bio-spherical cellulose nanofibres aerogels are prepared by chemical mechanic method, whose raw materials come from industrial and agricultural waste like waste newspapers, straw. Then, these biological materials are used for environmental treatment, such as industrial waste gas, and the obtained CO_2 was reapplied to industrial and agricultural production. These materials apply to sustainable development requirements and have great potential for development in the future.

Conclusions

In this article, we developed high-porosity, ultra-lightweight amino-modified bio-spherical cellulose nanofibres aerogels using a simple and highly efficient procedure based on the formation of C–O–Si bonds between cellulose nanofibres and AEAPMDS as an amine modifier in water. The bio-spherical cellulose nanofibres aerogels were easily prepared by freeze-drying spherical cellulose nanofibres hydrogels into which the amine group had been successfully introduced via the link to AEAPMDS. The cellulosic 3D structures obtained were mainly composed of fibre silk and thin sheets interconnected with nanofilaments covered by AEAPMDS. Compared with conventional inorganic porous carbon dioxide adsorbents, the amino-modified bio-spherical cellulose nanofibres aerogels showed excellent thermal stability and high *N* content (5.482%), displayed a high absorption capacity towards carbon dioxide (up to 1.78 mmol/g) and good regeneration (10 cycles), would not bring secondary pollution, and is composed of low-cost raw materials which could be produced from a broad variety of cellulose sources (including agricultural wastes or recycled paper). This work demonstrated the potential of amination to functionalize spherical cellulose nanofibres aerogels for CO_2 absorption and to give them multifunctional attributes. A wide library of functional amination is commercially available. Accordingly, this versatile functionalization method should open new opportunities for the design of novel advanced functional biomaterials with controlled properties. This new material showed an interesting application value in the field of CO_2 capture.

Acknowledgements This work was financially supported by the Special Fund for Forest Scientific Research in the Public Welfare (201504603), the Priority Academic Program Development (PAPD) of Jiangsu Higher Education Institutions, and the Doctorate Fellowship Foundation of Nanjing Forestry University of China (163020772).

References

Abdelmouleha M, Boufia S, Belgacemb MN, Duartec AP, Salaha AB, Gandinib A (2004) Modification of cellulosic fibres with functionalised silanes: development of surface properties. Int J Adhes Adhes 24:43–54. https://doi.org/10.1016/S0143-7496(03)00099-X

Aulin C, Varga I, Claesson PM, Wågberg L, Lindström T (2008) Buildup of polyelectrolyte multilayers of polyethyleneimine and microfibrillated cellulose studied by in situ dual-polarization interferometry and quartz crystal microbalance with dissipation. Langmuir ACS J Surf Colloids 24:2509–2518. https://doi.org/10.1021/la7032884

Bacsik Z, Ahlsten N, Ziadi A, Zhao G, Garciabennett AE, Martín-matute B, Hedin N (2011) Mechanisms and kinetics for sorption of CO_2 on bicontinuous mesoporous silica modified with *n*-propylamine. Langmuir ACS J Surf Colloids 27:11118–11128. https://doi.org/10.1021/la202033p

Cai J, Kimura S, Wada M, Kuga S, Zhang L (2008) Cellulose aerogels from aqueous alkali hydroxide–urea solution. Chemsuschem 1(1–2):149. https://doi.org/10.1002/cssc.200700039

Cervin NT, Aulin C, Larsson PT, Wågberg L (2012) Ultra porous nanocellulose aerogels as separation medium for mixtures of oil/water liquids. Cellulose 19:401–410. https://doi.org/10.1007/s10570-011-9629-5

Chakraborty AK, Bischoff KB, Astarita G, Damewood JR (2002) Molecular orbital approach to substituent effects in amine–CO_2 interactions. J Am Chem Soc 110:6947–6954. https://doi.org/10.1021/ja00229a003

Chen Z, Deng S, Wei H, Wang B, Huang J, Gang Y (2013) Polyethylenimine-impregnated resin for high CO_2 adsorption: an efficient adsorbent for CO_2 capture from simulated flue gas and ambient air. ACS Appl Mater Interfaces 5(15):6937–6945. https://doi.org/10.1021/am400661b

Chen W, Li Q, Wang Y, Yi X, Zeng J, Yu H, Liu Y, Li J (2014) Comparative study of aerogels obtained from differently prepared nanocellulose fibers. ChemSusChem 7(1):154–161. https://doi.org/10.1002/cssc.201300950

Chen SJ, Fu Y, Huang YX, Tao ZC, Zhu M (2016) Experimental investigation of CO_2 separation by adsorption methods in natural gas purification. Appl Energy 179:329–337. https://doi.org/10.1016/j.apenergy.2016.06.146

Danon A, Stair PC, Weitz E (2016) FTIR study of CO_2 adsorption on amine-grafted SBA-15: elucidation of adsorbed species. J Phys Chem C 115:11540–11549. https://doi.org/10.1021/jp200914v

Fischer F, Rigacci A, Pirard R, Berthon-Fabry S, Achard P (2006) Cellulose-based aerogels. Polymer 47:7636–7645. https://doi.org/10.1016/j.polymer.2006.09.004

Fu J, Wang S, He C, Lu Z, Huang J, Chen Z (2016) Facilitated fabrication of high strength silica aerogels using cellulose nanofibrils as scaffold. Carbohyd Polym 147:89–96. https://doi.org/10.1016/j.carbpol.2016.03.048

Ganster J, Fink HP (2003) Physical constants of cellulose. Wiley, New York. https://doi.org/10.1002/0471532053.bra036

Gavillon R, Budtova T (2008) Aerocellulose: new highly porous cellulose prepared from cellulose–NaOH aqueous solutions. Biomacromolecules 9(1):269–277. https://doi.org/10.1021/bm700972k

Gebald C, Wurzbacher JA, Tingaut P, Zimmermann T, Steinfeld A (2011) Amine-based nanofibrillated cellulose as adsorbent for CO_2 capture from air. Environ Sci Technol 45:9101–9108. https://doi.org/10.1021/es202223p

Hiyoshi N, Yogo K, Yashima T (2005) Adsorption of carbon dioxide on aminosilane-modified mesoporous silica. J Jpn Pet Inst 48:29–36. https://doi.org/10.1627/jpi.48.29

Huang HJ, Yuan WK, Chen XD (2006) Microencapsulation based on emulsification for producing pharmaceutical products: a literature review. Asia Pac J Chem Eng 14:515–544. https://doi.org/10.1002/apj.5500140318

Jin H, Nishiyama Y, Wada M, Kuga S (2004) Nanofibrillar cellulose aerogels. Colloids Surf A 240:63–67. https://doi.org/10.1016/j.colsurfa.2004.03.007

Jin C, Han S, Li J, Sun Q (2015) Fabrication of cellulose-based aerogels from waste newspaper without any pretreatment and their use for absorbents. Carbohyd Polym 123:150–156. https://doi.org/10.1016/j.carbpol.2015.01.056

Kerr RA (2007) Climate change—scientists tell policymakers we're all warming the world. Science 315:754–757. https://doi.org/10.1126/science.315.5813.754

Khatri RA, Chuang SSC, Soong Y, Gray M (2005) Carbon dioxide capture by diamine-grafted SBA-15: a combined fourier transform infrared and mass spectrometry study. Ind Eng Chem Res 44(10):3702–3708. https://doi.org/10.1021/ie048997s

Kim S, Ida J, Guliants V, Lin YS (2005) Tailoring surface properties of MCM-48 silica for selective adsorption of CO_2. J Phys Chem B 109:6287–6293

Kim J, Rubino I, Lee JY, Choi HJ (2016) Application of halloysite nanotubes for carbon dioxide capture. Mater Res Express 3(4):045019. https://doi.org/10.1088/2053-1591/3/4/045019

Knöfel C, Martin C, Hornebecq V, Llewellyn PL (2009) Study of carbon dioxide adsorption on mesoporous aminopropylsilane-functionalized silica and titania combining microcalorimetry and in situ infrared spectroscopy. J Phys Chem C 113:21726–21734. https://doi.org/10.1021/jp907054h

Lais A, Gondal MA, Dastageer MA (2017) Semiconducting oxide photocatalysts for reduction of CO_2 to methanol. Environ Chem Lett 2:1–28. https://doi.org/10.1007/s10311-017-0673-8

Liu FQ, Wang L, Huang ZG, Li CQ, Li W, Li RX, Li WH (2014) Amine-tethered adsorbents based on three-dimensional macroporous silica for CO(2) capture from simulated flue gas and air. ACS Appl Mater Interfaces 6(6):4371–4381. https://doi.org/10.1021/am500089g

Lu J, Askeland P, Drzal LT (2008) Surface modification of microfibrillated cellulose for epoxy composite applications. Polymer 49:1285–1296. https://doi.org/10.1016/j.polymer.2008.01.028

Lu W, Sculley JP, Yuan D, Krishna R, Zhou HC (2013) Carbon dioxide capture from air using amine-grafted porous polymer networks. J Phys Chem C 117:4057–4061. https://doi.org/10.1021/jp311512q

Mehmood K, Chang S, Yu S, Wang L, Li P, Li Z, Liu W, Rosenfeld D, Seinfeld JH (2017) Spatial and temporal distributions of air pollutant emissions from open crop straw and biomass burnings in China from 2002 to 2016. Environ Chem Lett. https://doi.org/10.1007/s10311-017-0675-6

Mohammed FS, Wuttigul S, Kitchens CL (2011) Dynamic surface properties of amino-terminated self-assembled monolayers incorporating reversible CO_2 chemistry. Ind Eng Chem Res 50:8034–8041. https://doi.org/10.1021/ie102526s

Niu M, Yang H, Zhang X, Wang Y, Tang A (2016) Amine-impregnated mesoporous silica nanotube as an emerging nanocomposite for CO_2 capture. ACS Appl Mater Interfaces 8(27):17312. https://doi.org/10.1021/acsami.6b05044

Plaza MG, Pevida C, Arenillas A, Rubiera F, Pis JJ (2007) CO_2 capture by adsorption with nitrogen enriched carbons. Fuel 86:2204–2212. https://doi.org/10.1016/j.fuel.2007.06.001

Rochelle GT (2009) Amine scrubbing for CO_2 capture. Science 325:1652–1654. http://www.jstor.org/stable/40301873

Roth EA, Agarwal S, Gupta RK (2013) Nanoclay-based solid sorbents for CO_2 capture. Energy Fuels 27:4129–4136. https://doi.org/10.1021/ef302017m

Sehaqui H, Salajková M, Zhou Q, Berglund LA (2010) Mechanical performance tailoring of tough ultra-high porosity foams prepared

from cellulose I nanofiber suspensions. Soft Matter 6:1824–1832. https://doi.org/10.1039/b927505c

Sehaqui H, Allais M, Zhou Q, Berglund LA (2011a) Wood cellulose biocomposites with fibrous structures at micro- and nanoscale. Compos Sci Technol 71:382–387. https://doi.org/10.1016/j.compscitech.2010.12.007

Sehaqui H, Zhou Q, Berglund LA (2011b) High-porosity aerogels of high specific surface area prepared from nanofibrillated cellulose (NFC). Compos Sci Technol 71:1593–1599. https://doi.org/10.1016/j.compscitech.2011.07.003

Sehaqui H, Becatinni V, Cheng NY, Steinfeld A, Zimmermann T, Tingaut P (2015) Fast and reversible direct CO_2 capture from air onto all-polymer nanofibrillated cellulose—polyethyleneimine foams. Environ Sci Technol 49(5):3167. https://doi.org/10.1021/es504396v

Sharma P, Baek IH, Park YW, Nam SC, Park JH, Park SD, Park SY (2012) Adsorptive separation of carbon dioxide by polyethyleneimine modified adsorbents. Korean J Chem Eng 29:249–262. https://doi.org/10.1007/s11814-011-0158-6

Shi J, Lu L, Guo W, Zhang J, Cao Y (2013) Heat insulation performance, mechanics and hydrophobic modification of cellulose–SiO_2 composite aerogels. Carbohyd Polym 98:282–289. https://doi.org/10.1016/j.carbpol.2013.05.082

Shlyakhtina AV, Oh YJ (2008) Transparent SiO_2 aerogels prepared by ambient pressure drying with ternary azeotropes as components of pore fluid. J Non Cryst Solids 354:1633–1642. https://doi.org/10.1016/j.jnoncrysol.2007.10.033

Silva TCF, Habibi Y, Colodette JL, Elder T, Lucia LA (2012) A fundamental investigation of the microarchitecture and mechanical properties of tempo-oxidized nanofibrillated cellulose (NFC)-based aerogels. Cellulose 19:1945–1956. https://doi.org/10.1007/s10570-012-9761-x

Svagan AJ, Samir MASA, Berglund LA (2008) Biomimetic foams of high mechanical performance based on nanostructured cell walls reinforced by native cellulose nanofibrils. Adv Mater 20:1263–1269. https://doi.org/10.1002/adma.200701215

Víctor-Román S, Simón-Herrero C, Romero A, Gracia I, Valverde JL, Sánchez-Silva L (2015) CNF-reinforced polymer aerogels: influence of the synthesis variables and economic evaluation. Chem Eng J 262:691–701. https://doi.org/10.1016/j.cej.2014.10.026

Vilarrasa-Garcia E, Moya EMO, Cecilia JA Jr, Cavalcante CL, Jiménez-Jiménez J, Azevedo DCS, Rodríguez-Castellón E (2015) CO_2 adsorption on amine modified mesoporous silicas: effect of the progressive disorder of the honeycomb arrangement. Microporous Mesoporous Mater 209:172–183. https://doi.org/10.1016/j.micromeso.2014.08.032

Xu X, Song C, Andrésen JM, Miller BG, Scaroni AW (2003) Preparation and characterization of novel CO_2 "molecular basket" adsorbents based on polymer-modified mesoporous molecular sieve MCM-41. Microporous Mesoporous Mater 62:29–45. https://doi.org/10.1016/S1387-1811(03)00388-3

Zhang X, Zheng X, Zhang S, Zhao B, Wu W (2012) AM-TEPA impregnated disordered mesoporous silica as CO_2 capture adsorbent for balanced adsorption–desorption properties. Ind Eng Chem Res 51:15163–15169. https://doi.org/10.1021/ie300180u

Zhang Z, Sèbe G, Rentsch D, Zimmermann T, Tingaut P (2014) Ultralightweight and flexible silylated nanocellulose sponges for the selective removal of oil from water. Geogr Res 26:2659–2668. https://doi.org/10.1021/cm5004164

Zhang Z, Wang H, Li S, Li L, Li D (2015) Transparent and flexible cellulose nanofibers/silver nanowires/acrylic resin composite electrode. Composites A 76:309–315. https://doi.org/10.1016/j.compositesa.2015.06.010

Zhang H, Liu R, Lal R (2016) Optimal sequestration of carbon dioxide and phosphorus in soils by gypsum amendment. Environ Chem Lett 14:443–448. https://doi.org/10.1007/s10311-016-0564-4

Zhao Y, Xu C, Xing C, Shi X, Matuana LM, Zhou H, Ma X (2015) Fabrication and characteristics of cellulose nanofibril films from coconut palm petiole prepared by different mechanical processing. Ind Crops Prod 65:96–101. https://doi.org/10.1016/j.indcrop.2014.11.057

Zheng Q, Cai Z, Gong S (2014) Green synthesis of polyvinyl alcohol (PVA)–cellulose nanofibril (CNF) hybrid aerogels and their use as superabsorbents. J Mater Chem A 2:3110–3118. https://doi.org/10.1039/c3ta14642a

Zheng Q, Zhang H, Mi H, Cai Z, Ma Z, Gong S (2016) High-performance flexible piezoelectric nanogenerators consisting of porous cellulose nanofibril (CNF)/poly(dimethylsiloxane) (PDMS) aerogel films. Nano Energy 26:504–512. https://doi.org/10.1016/j.nanoen.2016.06.009